Molecular dynamics to rationalize EXAFS experiments: a dynamical model explaining hydration behaviour across the lanthanoid(III) series

Riccardo Spezia[1], Magali Duvail[1], Pierre Vitorge[1,2], and Paola D'Angelo[3]

[1]LAMBE UMR 8587 CNRS, Université d'Evry Val d'Essonne, Bd F. Mitterrand, 91025 Evry Cedex

[2]CEA Saclay, DEN/DPC/SECR/LSRM

[3]Dipartimento di Chimica, Universitá di Roma "La Sapienza"

E-mail: `riccardo.spezia@univ-evry.fr`

Abstract. In this paper we show how polarizable molecular dynamics can be successfully used to understand lanthanoid(III) (Ln) hydration. In particular, our modelling is in very good agreement with EXAFS data and thus the microscopic picture emerging directly from dynamics can be useful to understand experiments. We show three examples across the series: at the beginning (Nd^{3+}), middle (Gd^{3+}) and end (Yb^{3+}). Using these examples, we show that we are able to reproduce not only Ln-oxygen distances but also the changeover in coordination number across the series. The peculiarity of the changeover of lanthanoid coordination number in the middle of the series emerges from high exchange frequency, such that a molecular dynamics approach becomes a fundamental tool to understand this phenomenon.

1. Introduction

Understanding hydration around heavy metal cations – like transition metals, lanthanoids or actinoids – is of fundamental importance to address their physical and chemical properties in water. For aqueous solutions the first step is to understand solvation properties. Molecular dynamics (MD) simulations can provide a real help in understanding the molecular structure of hydrated ions as a method to better interpret X-ray absorption experiments. In particular in last years, the coupling between EXAFS experiments and molecular dynamics was a very powerful tool to build up a complete picture of the hydration process of different metal cations [1, 2, 3, 4]. EXAFS can provide accurate information on the metal-water distances while microscopic simulations give details on the structure. Further, simulations can give insights into the dynamical properties, i.e. metal-water vibrations and water self-exchange dynamics.

Among hydrated metals, lanthanoids(III), Ln^{3+}, belong to a chemical series with similar chemical reactivity presenting a changeover of water coordination number (CN) across the series: light lanthanoids have CN=9 while heavier – actually smaller – ones have CN=8. Since the mid-1960's this changeover was modelled via the so called gadolinium break model [5, 6, 7, 8, 9]. Recently, this model was revised via experimental and theoretical studies showing that the changeover occurs in a continuous way [10, 11, 12, 13, 14], reflecting the difference in exchange dynamics across the series. In particular, MD simulations and EXAFS analysis were fundamental

to clarify the modification of hydration across the lanthanoid(III) series. These studies were conducted independently, leading to qualitatively similar conclusions [11, 12].

Recently, we have developed a polarizable water-lanthanum potential [15] providing very good results when directly compared with EXAFS data [16]. This polarization potential was then extended to the whole series providing probably the classical interaction potential that better agrees with experimental structural data. After the first pioneering work of Kowall et al. [17, 18], recently classical [14, 19], DFT-based [20, 21] and QM/MM [22] simulations are reported in the litterature on different Ln^{3+} giving insights into some selected atoms along the series but never studying the whole series in details. Further, they do not reproduce always Ln-O and Ln-H distances and coordination numbers with the needed accuracy. An accurate comparison between experimental EXAFS signals and theoretical microscopic structural and dynamical data is still lacking. In this work we have coupled MD simulations and EXAFS data for three ions: Nd^{3+}, Gd^{3+} and Yb^{3+}. We have chosen those atoms since they are representative of the series, being at the beginning (Nd^{3+}), middle (Gd^{3+}) and end (Yb^{3+}).

2. Methods

2.1. Molecular simulations

Molecular dynamics was carried out immersing each Ln^{3+} ion in a box containing 216 water molecules without counter-anions. The system was neutralizing by a neutralizing plasma in the Ewald summation. Periodic boundary conditions were applied to mimic bulk conditions. Simulations were done using the velocity-Verlet-based multiple time scale algorithm. Equation of motions were numerically integrated with a 1 fs time step. Each system was first equilibrated at 298 K for 2 ps and subsequently the production runs were propagated for 3 ns in the NVE ensemble. All details on molecular simulation runs and polarizable interaction potential are the same as reported previously [12, 13, 15, 23].

2.2. EXAFS measurements and data analysis

The aqueous solutions of the lanthanoid ions were made by dissolving a weighed amount of hydrated trifluoromethanesulfonates in freshly distilled water. The concentration of the samples was 0.2 M and the solutions were acidified to about pH=1 by adding trifluoromethanesulforic acid to avoid hydrolysis. The added H^+_{aq} cations are statistically far enough from Ln^{3+}_{aq} to have a negligible influence on its EXAFS signal. The corresponding added anion is known to be non complexing in such conditions. The K-edge spectra were collected at ESRF, on the bending magnet X-ray-absorption spectroscopy beam line BM29 [26] in transmission geometry.

For disordered systems the $\chi(k)$ signal is represented by the equation:

$$\chi(k) = \int_0^\infty dr \ 4\pi\rho r^2 g(r) A(k,r) \sin\left[2kr + \phi(k,r)\right] \tag{1}$$

where $A(k,r)$ and $\phi(k,r)$ are the amplitude and phase functions, respectively, and ρ is the density of the scattering atoms. A direct comparison between MD and EXAFS results can be performed by calculating the $\chi(k)$ theoretical signal associated with the MD Ln-O and Ln-H $g(r)$'s and by comparing it with the experimental spectrum, without carrying out any minimization procedure. Both Ln-O and Ln-H $g(r)$'s have been used to calculate the single scattering first shell $\chi(k)$ theoretical signal, because the Ln-hydrogen interactions can provide a detectable contribution to the EXAFS spectra, as found in the case of transition-metal ions and La^{3+} in aqueous solutions [1, 16, 27]. The $\chi(k)$ theoretical signals have been calculated by means of the GNXAS program [28] and a thorough description of this procedure can be found in Ref. [1, 29]. In the analysis, the S_0^2 parameter, which accounts for an overall intensity rescaling, and E_0 which aligns the experimental and theoretical energy scales were taken from the results

Table 1. Hydration properties obtained by molecular dynamics simulations compared with literature experimental and theoretical data available. $r_{Ln-O}^{(1)}$, $CN^{(1)}$ and $MRT^{(1)}$ are respectively the Ln-O distance (in Å), the coordination number and the mean residence time (in picoseconds) of the first hydration shell.

Method	$r_{Ln-O}^{(1)}$	$CN^{(1)}$	$MRT^{(1)}$
Nd^{3+}			
P-CLMD[a]	2.48	9.00	1482
EXAFS[b]	2.49	9.0	
EXAFS[c]	2.50	9	
MCDHO[d]	2.63	8.9	1204-1818
CLMD[e]	2.53	9.17	
Gd^{3+}			
P-CLMD[a]	2.44/2.39	8.95/8.72	426/254
EXAFS[b]	2.41	8.0	
EXAFS[c]	2.39	9	
MCDHO[d]	2.55	8.4	552-621, 319
CLMD[e]	2.46	8.99	
Yb^{3+}			
P-CLMD[a]	2.36/2.32	8.33/8.02	227/665
EXAFS[b]	2.32	8.0	
EXAFS[c]	2.34	8.7	
MCDHO[d]	2.47	8.0	8333-16667, 493
CLMD[e]	2.37	9.01	

[a] Polarizable classical molecular dynamics of this work. Left $Ln_{(9)}^{3+}$ results, right $Ln_{(8)}^{3+}$ results, when available (Gd^{3+} and Yb^{3+}). [b] EXAFS from Refs. [24, 25]. [c] EXAFS from Ref. [11]. [d] Polarizable molecular dynamics using the MCDHO model reported on Ref. [14]. MRT are calculated from water-exchange rate constants $MRT = 1/k_{ex}$. [e] Molecular dynamics simulation with interaction parameters fitted on ab-initio results reported in Ref. [19].

reported in Ref. [30]. Notably, $S_0^2 = 0.99$ for all species and E_0 values are 43567 ± 0.5 eV, 50243 ± 1 eV and 61337 ± 1 eV for Nd, Gd and Yb respectively.

3. Results
Main structural and dynamical properties of polarizable classical molecular dynamics (P-CLMD) are reported in Table 1 where Ln-O distances, Ln-water coordination numbers and first shell water mean residence times are compared with available data reported in the literature. In Figure 1 we show Ln-O and Ln-H radial distribution functions obtained for three case systems. Our Nd^{3+}-O distance of 2.48 Å is in good agreement with experimental structural data available in the literature [11, 24, 25] (2.49 and 2.50 Å, see Table 1), better than other simulations both polarizable [14] (2.63 Å) and non-polarizable [19] (2.53 Å). Also mean residence time, for which experimental data are only present for H_2O-SO_4^{2-}, are in good agreement with experiments providing values less than 2 ns [10] and in a similar range of recent simulation results [14]. However, a direct proof of the reliability of our MD results has been obtained by comparing the theoretical EXAFS spectrum calculated from the Nd-O and Nd-H g(r)'s with the experimental
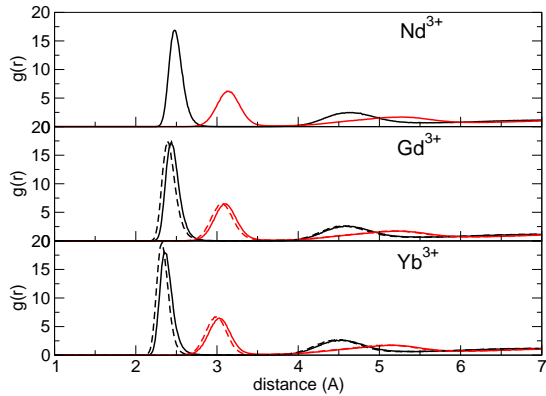
Figure 1. Radial distribution functions, Ln-O in black and Ln-H in red, obtained using $Ln^{3+}_{(9)}$, solid lines, and $Ln^{3+}_{(8)}$, dashed lines.
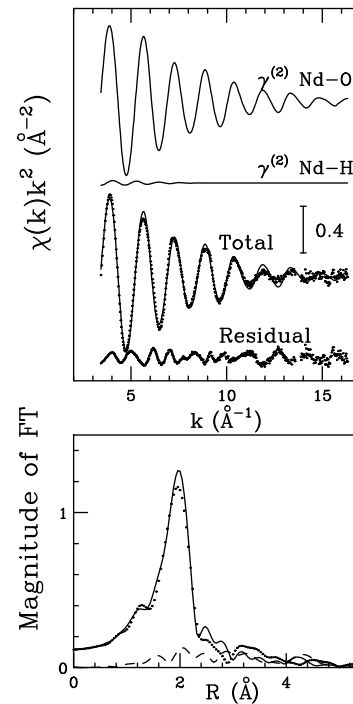

Figure 2. Analysis of the K-edge EXAFS spectrum of aqueous solutions of Nd^{3+} starting from the Nd-O and Nd-H radial distribution functions obtained from MD simulations (solid lines). Experimental data curves are in dotted lines.

data without carrying out any structural minimization. The agreement between the theoretical and experimental spectra is a direct strict test of the accuracy of the MD simulations. In the upper panel of Figure 2 the comparison between the EXAFS experimental signal and the theoretical curves is reported for the Nd^{3+} ion. The $\gamma^{(n)}$ signals are shown multiplied by k squared for better visualization. The first two curves from the top are the Nd-O and Nd-H first shell $\gamma^{(2)}$ contributions while the reminder of the figure shows the total theoretical contribution compared with the experimental spectrum and the resulting residuals. As expected, the dominant contribution to the total EXAFS spectrum is given by the Nd-O first shell signal and, as a consequence, the EXAFS structural information is particularly accurate for the shape of the Ln-O $g(r)$'s first peak, only. The Fourier transform (FT) moduli of the EXAFS $\chi(k)k^2$ theoretical, experimental and residual signals are shown in the lower panels of Figure 2. The FT has been calculated in the k-range 3.5-15.0 Å^{-1} with no phase shift correction applied. Both the EXAFS and FT theoretical signals match the experimental data very well showing that the structural and dynamical information derived from the MD simulations is basically correct.

For Gd^{3+} and Yb^{3+} we report data obtained with two sets of parameters, $Ln^{3+}_{(9)}$ obtained from ionic radii corresponding to CN=9 and $Ln^{3+}_{(8)}$ obtained from ionic radii corresponding to CN=8. Inspection of Table 1 shows that for Yb^{3+} the $Ln^{3+}_{(8)}$ parameters reproduce better previously reported experiments [11, 24, 25]: the 2.32 Å $Yb^{3+}_{(8)}$-O distance is typically in better agreement with the 2.32-2.34 Å published EXAFS distances than the 2.36 Å $Yb^{3+}_{(9)}$-O distance.

Also in this case our results are in better agreement with reported experiments than other simulations [14, 19].

For Gd^{3+} the situation is less clear. $Gd^{3+}_{(8)}$ distances (2.39 Å) seem to reproduce better experimental distances (2.41-2.39 Å) reported previously [11, 24, 25], but dynamical exchange seems to be too fast. We will thus compare directly EXAFS signal obtained from $Gd^{3+}_{(9)}$ and $Gd^{3+}_{(8)}$ simulations with experimental one.
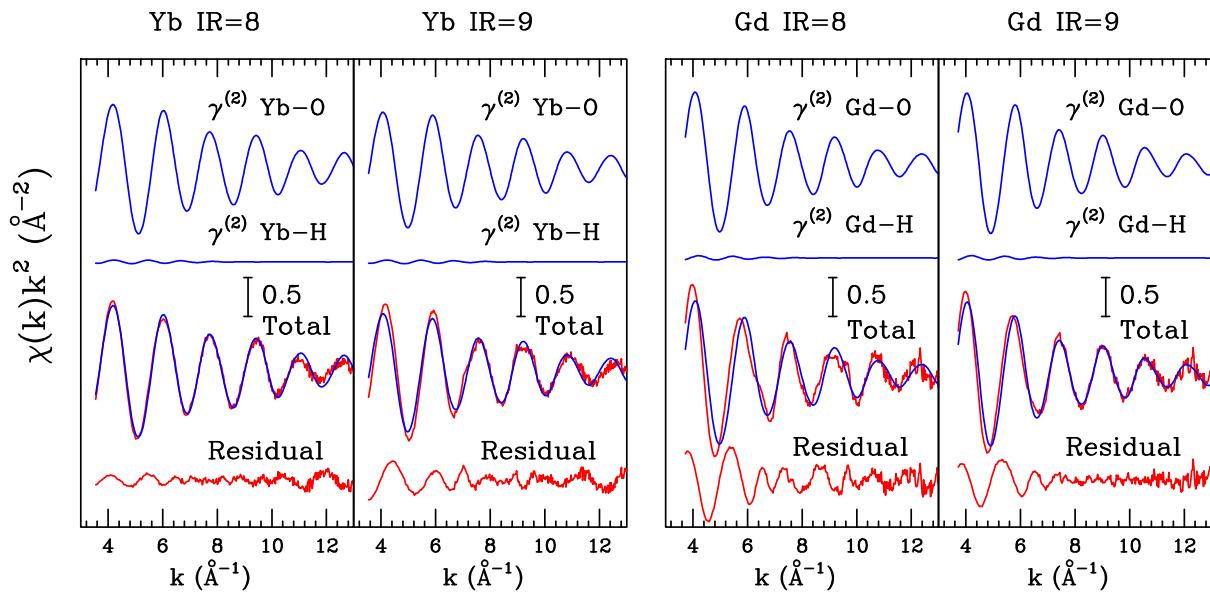

Figure 3. Analysis of the K-edge EXAFS spectra of aqueous solutions of Yb^{3+} (left panel) and Gd^{3+} (right panel), starting from the Ln-O and Ln-H radial distribution functions obtained from MD simulations carried out with different ionic radii (in blue). Experimental data curves are in red.

We have directly compared the EXAFS theoretical signals obtained from our simulations with the experimental spectra also for Yb^{3+} and Gd^{3+} as shown in Figure 3. For Yb^{3+} the simulation performed with the $Yb^{3+}_{(8)}$ parametes is in very good agreement with the experimental data while a slight mismatch has been found for the $Yb^{3+}_{(9)}$ simulation. Note that in the former simulation the Yb^{3+} hydration complexes are formed on average by eight water molecules, in agreement with previous experimental determinations [11]. A less defined result has been obtained for the Gd^{3+} ion. In this case, even if a better agreement is found for the $Gd^{3+}_{(9)}$ parameters by a direct comparison of theoretical and experimental EXAFS signal as in Figure 3, neither simulation is in perfect agreement with the EXAFS experimental data. We should remember that paramters are directly linked with ionic radii and, indirectly, with coordination numbers. Thus, it not so surprisingly that for atoms for which in solution we have a statistical coexistence of two CNs – and thus of two effective ionic radii – the best set of parameters should be in between $Ln^{3+}_{(9)}$ and $Ln^{3+}_{(8)}$ ones. All together these findings demonstrate the reliability of our polarizable simulations.

4. Conclusions
In this work we have shown that molecular dynamics simulations including polarization are able to correctly reproduce EXAFS experimental data. For Nd^{3+} and Yb^{3+} the CN=9 and CN=8

parameters, respectively, better reproduce previously reported EXAFS experiments [11, 24, 25] as well as the EXAFS experimental data presented in this work. These parameters correspond also to the coordination numbers that are predominant for the two ions: the 9-folded for Nd^{3+}, as for ions at the beginning of the series, and the 8-folded coordination for Yb^{3+}, as for ions at the end of the series. For Gd^{3+} the (8) potential that provides distances in better agreement with data reported in the literature, seems to work worst than the (9) potential when accurately compared with EXAFS experimental signal. As a consequence, the coordination number seems to be higher, closer to 9 than 8, and the first shell water mean residence time should be closer to 400 ps than to 200 ps as reported by the (8) potential. Thus, the CN curve across the series reported in Ref. [12] can be shifted towards heavier elements. A more detailed study seems to be needed, considering more elements and also XANES measurements recently obtained [31]. These results can be also a guide to design an optimal set of parameters that can fully catch structural and dynamical data for the middle of the series. We should note that for the beginning and the end of the series these parameters, based upon MP2 calculations on La^{3+} and then extended for the whole series just taking into account atomic properties like ionic radii and polarizabilities, reproduce very accurately experimental data even when a direct comparison of associated EXAFS signals is performed as in the present work.

References

[1] D'Angelo P, Barone V, Chillemi G, Sanna N, Mayer-Klaucke W and Pavel N V 2002 *J. Am. Chem. Soc.* **124** 1958–1967

[2] Chillemi G, D'Angelo P, Pavel N V, Sanna N and Barone V 2002 *J. Am. Chem. Soc.* **124** 1968–1976

[3] Spezia R, Duvail M, Vitorge P, Cartailler T, Tortajada J, D'Angelo P and Gaigeot M-P 2006 *J. Phys. Chem. A* **110** 13081–13088

[4] D'Angelo P, Migliorati V, Mancini G, Barone V and Chillemi G 2008 *J. Chem. Phys.* **128** 84502

[5] Habenschuss A and Spedding F H 1979 *J. Chem. Phys.* **70** 2797–2806

[6] Habenschuss A and Spedding F H 1979 *J. Chem. Phys.* **70** 3758–3763

[7] Choppin G R and Strazik W F 1965 *Inorg. Chem.* **4** 1250–1254

[8] Choppin G R and Graffeo A J 1965 *Inorg. Chem.* **4** 1254–1257

[9] Bertha S L and Choppin G R 1969 *Inorg. Chem.* **8** 613–617

[10] Helm L and Merbach A E 2005 *Chem. Rev.* **105** 1923–1960

[11] Persson I, D'Angelo P, De Panfilis S, Sandstrom M and Eriksson L 2008 *Chem. Eur. J.* **14** 3056–3066

[12] Duvail M, Spezia R and Vitorge P 2008 *ChemPhysChem.* **9** 693–696

[13] Duvail M, Vitorge P and Spezia R 2009 *J. Chem. Phys.* **130** 104501

[14] Villa A, Hess B and Saint-Martin H 2009 *J. Phys. Chem. B* **113** 7270–7281

[15] Duvail M, Souaille M, Spezia R, Cartailler T and Vitorge P 2007 *J. Chem. Phys.* **127** 034503

[16] Duvail M, D'Angelo P, Gaigeot M-P, Vitorge P and Spezia R 2009 *Radiochim. Acta* **97** 339–346

[17] Kowall T, Foglia F, Helm L and Merbach A E 1995 *J. Phys. Chem.* **99** 13078–13087

[18] Kowall T, Foglia F, Helm L and Merbach A E 1995 *J. Am. Chem. Soc.* **117** 3790–3799

[19] Floris F M and Tani A 2001 *J. Chem. Phys.* **115** 4750–4765

[20] Ikeda T, Hirata M and Kimura T 2005 *J. Chem. Phys.* **122** 244507

[21] Yazyev O V and Helm L 2007 *J. Chem. Phys.* **127** 084506

[22] Hofer T S, Scharnagl H, Randolf B R and Rode B M 2006 *Chem. Phys.* **327** 31–42

[23] Duvail M, Spezia R, Cartailler T and Vitorge P 2007 *Chem. Phys. Lett.* **448**(1-3) 41–45

[24] Ishiguro S I, Umebayashi Y, Kato K, Takahashib R and Ozutsumi K 1998 *J. Chem. Soc. Faraday Trans.* **94** 3607–3612

[25] Ishiguro S I, Umebayashi Y and Komiya M 2002 *Coord. Chem. Rev* **226** 103–111

[26] Filipponi A, Borowski M, Bowron D T, Ansell S, De Panfilis S, Di Cicco A and Itiè J-P 2000 *Rev. Sci. Instrum.* **71**, 2422–2432

[27] Filipponi A, D'Angelo P, Pavel N V and Di Cicco A 1994 *Chem. Phys. Lett.* **225** 150–155

[28] Filipponi A, Di Cicco A and Natoli C R 1995 *Phys. Rev. B* **52** 15122

[29] Burattini E, D'Angelo P, Giglio E and Pavel N V 1991 *J. Phys. Chem.* **95**, 7880–7885

[30] D'Angelo P, De Panfilis S, Filipponi A and Persson I 2008 *Chem.-Eur. J.* **14**, 3045–3055

[31] D'Angelo P, *personal communication*